

Exploring Iterative Refinement with Diffusion Models for Video Grounding

Xiao Liang^{1*}, Tao Shi^{1*}, Yaoyuan Liang¹, Te Tao¹, Shao-Lun Huang^{1†}

¹Shenzhen International Graduate School, Tsinghua University
 {liangx22, shitao21, liang-yy21, taot22}@mails.tsinghua.edu.cn, shaolun.huang@sz.tsinghua.edu.cn

Abstract

Video grounding aims to localize the target moment in an untrimmed video corresponding to a given sentence query. Existing methods typically select the best prediction from a set of predefined proposals or directly regress the target span in a single-shot manner, resulting in the absence of a systematical prediction refinement process. In this paper, we propose DiffusionVG, a novel framework with diffusion models that formulates video grounding as a conditional generation task, where the target span is generated from Gaussian noise inputs and iteratively refined in the reverse diffusion process. During training, DiffusionVG progressively adds noise to the target span with a fixed forward diffusion process and learns to recover the target span in the reverse diffusion process. In inference, DiffusionVG can generate the target span from Gaussian noise inputs by the learned reverse diffusion process conditioned on the video-sentence representations. Our DiffusionVG follows the encoder-decoder architecture, which firstly encodes the video-sentence features and iteratively denoises the predicted spans in its specialized span refining decoder. Without bells and whistles, our DiffusionVG demonstrates competitive or even superior performance compared to existing well-crafted models on mainstream Charades-STA and ActivityNet Captions benchmarks. Our code will be available at [this url](https://this.url).

Introduction

Video grounding (VG) is a fundamental task in video-language understanding, which focuses on identifying the start and end timestamps of a target moment (termed as target span) that exhibits the highest semantic correspondence with a sentence query in an untrimmed video. As shown in Fig 1(a), this task is challenging since it requires not only separate understanding of the video and sentence representations but also comprehension of their corresponding interaction. Recently, VG has attracted increasing attention from the multimedia community (Gao et al. 2017; Zhang et al. 2022) due to its wide range of applications, including video question answering (Ye et al. 2017; Lei et al. 2018) and video editing (Fu et al. 2022).

The majority of existing methods on VG can be generally classified into two primary categories: (1) Proposal-based

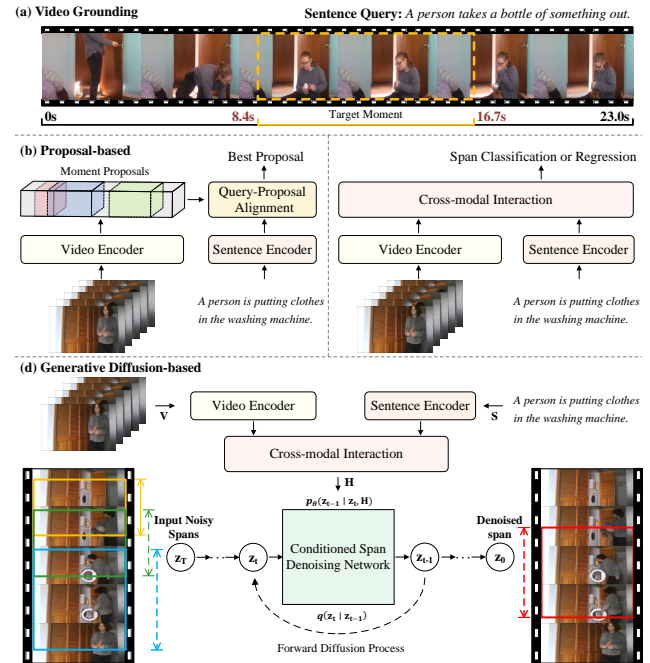


Figure 1: (a) An illustration of the video grounding task, which aims to locate a target moment that semantically corresponds to a sentence query in a video. (b) The pipeline of proposal-based VG methods. (c) The pipeline of proposal-free VG methods. (d) An illustration of our proposed DiffusionVG, which formulates VG as a conditional generative task with diffusion models.

methods (Gao et al. 2017; Xu et al. 2018; Xiao et al. 2022; Zhang et al. 2020b; Liu et al. 2021): Following the propose-and-rank pipeline, these methods first generate a group of moment proposals with predefined multi-scale anchors, then predict alignment scores for each proposal after aggregating contextual multi-modal information to identify the optimal matching moment, as depicted in Fig. 1(b). (2) Proposal-free methods (Zeng et al. 2020; Li, Guo, and Wang 2021; Zhao et al. 2021; Tang et al. 2022; Zhang et al. 2021a): As shown in Fig. 1(c), these methods directly regress the start and end timestamps from each frame or predict the probabilities for each frame to serve as the start and end frame.

Although both groups of methods have achieved promis-

*These authors contributed equally.

† Corresponding author.

ing performance, they are still plagued by several significant limitations: (1) In proposal-based methods, the performance heavily relies on both the quantity and quality of predefined anchors, thereby imposing a substantial computational cost arising from the redundant proposal generation and matching processes. (2) For proposal-free methods, incorporating frame-wise predictions poses challenges in optimization as the extensive search space for moment prediction, which results in inferior performance. (3) All these methods employ a single-shot prediction strategy, neglecting a fundamental procedure for refining the initial prediction and resulting in suboptimal target moment localization.

Inspired by the inherent attributes of the multi-step denoising process in diffusion models (Sohl-Dickstein et al. 2015; Ho, Jain, and Abbeel 2020; Chen et al. 2022a; Rombach et al. 2022), this paper presents DiffusionVG, a novel framework that employs diffusion models to formulate VG as a conditional generative task. The central motivation for DiffusionVG is to enable the iterative refinement of the predicted target span through the advantage of denoising diffusion. As illustrated in Fig. 1(d), the predicted target span in DiffusionVG is generated from Gaussian noise inputs conditioned on the video-sentence representations through the reverse diffusion process. During training, we systematically add Gaussian noise with a predefined variance schedule to the ground-truth span in the forward diffusion process, resulting in the production of noisy spans. Subsequently, a denoising network is learned to recover the original target span, conditioned on the video-sentence representations obtained from a multi-modal encoder. At inference stage, once the video-sentence representations are encoded, DiffusionVG generates the initial predicted spans from Gaussian noise inputs and iteratively refines the predictions through the learned reverse diffusion process. To determine the best prediction among all generated spans, we employ a voting strategy to select the final prediction.

Specifically, DiffusionVG utilizes an encoder-decoder architecture (Vaswani et al. 2017), wherein a video-centered multi-modal encoder facilitates the interaction between video and sentence features and a specialized span refining decoder is employed for generating the target span. In contrast to aforementioned methods, our proposed DiffusionVG eliminates the need for predefined anchors and concentrates all queries (noisy spans) on recovering a single target span, which significantly simplifies the optimization. Moreover, once the DiffusionVG is trained, it has the flexibility to utilize any number of denoising sampling steps and queries in inference, irrespective of the configuration in the training stage. This adaptability of DiffusionVG allows for optimizing the accuracy of target moment localization while maintaining a balance with inference speed.

To demonstrate the effectiveness of DiffusionVG, we conduct extensive experiments on both Charades-STA (Gao et al. 2017) and ActivityNet Captions (Krishna et al. 2017) datasets. Without bells and whistles, our DiffusionVG surpasses all existing well-designed state-of-the-art methods on Charades-STA across all evaluation metrics and achieves competitive performance on ActivityNet Captions. To further illustrate the effectiveness of the iterative refinement in

DiffusionVG, we conduct a comparison with a Transformer-based model (Carion et al. 2020) using identical parameter settings, with the exception of the learnable queries and classification module in the latter. Results showcased in Tab. 2 provide compelling evidence of DiffusionVG’s superiority over standard Transformer models in VG.

Our **contributions** can be summarized as: (1) We innovatively formulate video grounding as a conditional generative task using diffusion models, enabling iterative refinement of predicted spans through the reversed denoising diffusion process. (2) We further design a video-centered encoder and a span refining decoder for our proposed DiffusionVG to optimize its compatibility with the VG task and enhance performance. (3) Extensive experiments on both Charades-STA and ActivityNet Captions benchmarks demonstrate that DiffusionVG achieves competitive or even superior performance against existing state-of-the-arts.

Related Work

Video Grounding (VG)

As introduced by (Gao et al. 2017; Hendricks et al. 2017), this task aims to retrieve a target moment from an untrimmed video that semantically corresponds to a given sentence query. To achieve precise localization of the desired moment via language descriptions, it is essential for a VG model to establish the semantic alignment between the video and sentence inputs. Early methods mainly resort to the propose-and-rank pipeline (Gao et al. 2017; Xu et al. 2018; Zhang et al. 2020b; Xiao et al. 2022; Zhang et al. 2019; Chen and Jiang 2019; Ge et al. 2018; Chen et al. 2018; Liu et al. 2020, 2018; Qu et al. 2020; Wang, Ma, and Jiang 2019; Yuan et al. 2022; Zhang et al. 2019, 2021b; Liu et al. 2021; Wang et al. 2021), which produce a set of moment proposals with predefined multi-scale anchors in the initial stage. After aggregating contextual multi-modal information, the model can predict alignment scores for each proposal and find the best matching moment. While these proposal-based methods provide reliable results, they have to perform cumbersome proposal generation and pair all proposals with the given query, which contribute to heavy computation cost. In contrast, recently proposal-free methods (Yuan, Mei, and Zhu 2019; Chen et al. 2020a,b; Li, Guo, and Wang 2021; Chen and Jiang 2020; Mun, Cho, and Han 2020; Wang et al. 2020; Wang, Ma, and Jiang 2020; Zeng et al. 2020; Zhang et al. 2020a, 2021a; Nan et al. 2021; Tang et al. 2022) have been developed to directly regress the start and end timestamps or estimate the probabilities for each frame to be the start and end frame, which can efficiently avoid the time-consuming proposal generating and ranking processes. Despite the efficiency advantages of the proposal-free methods, the integration of frame-wise predictions presents optimization challenges from the extensive search space, making these methods result in inferior performance. In contrast to existing methods, this paper presents DiffusionVG, an innovative framework that pioneers the exploration of diffusion-based generative models in VG, as illustrated in Fig. 1(d).

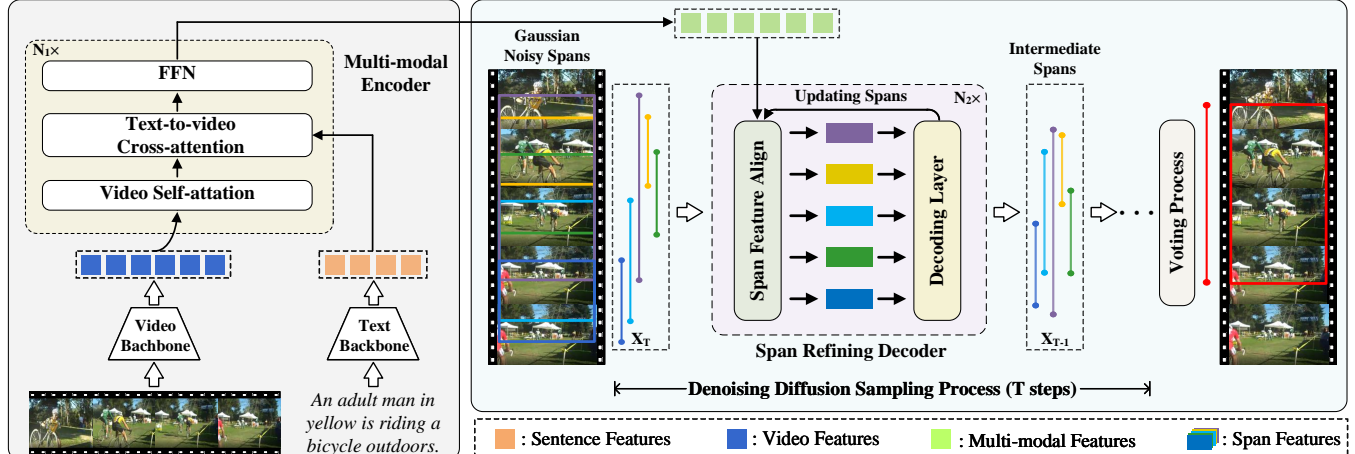


Figure 2: Overview of DiffusionVG. Taking a video and a sentence query as input, DiffusionVG first extracts features from both modalities and facilitates interaction using a video-centered multi-modal encoder. Subsequently, the predictions of the target span are generated in a span refining decoder conditioned on the encoded multi-modal representations and iteratively refined through the reverse diffusion process. The final prediction of the target span is selected via a voting process.

Diffusion Model

Originally introduced in (Sohl-Dickstein et al. 2015) and improved by (Song and Ermon 2019; Ho, Jain, and Abbeel 2020; Song et al. 2021), diffusion models consist of a forward diffusion process (add noises to data) and a reverse denoising process (recover data from noises). Due to the robust generation and generalization capabilities, diffusion models have exhibited remarkable achievements in the fields of both computer vision (Fan et al. 2023; Saharia et al. 2022; Harvey et al. 2022; Yang, Srivastava, and Mandt 2022; Rombach et al. 2022; Dhariwal and Nichol 2021; Gu et al. 2022; Nichol et al. 2021; Zhang and Agrawala 2023) and natural language processing (Austin et al. 2021; Gong et al. 2022; Li et al. 2022; Shen et al. 2023; Strudel et al. 2022).

The majority of studies on diffusion models focus on their generative aspects, overlooking their discriminative capability on perception tasks. Some pioneer studies (Baranchuk et al. 2021; Wolleb et al. 2022; Amit et al. 2021) have attempted to employ diffusion models for image segmentation tasks. (Chen et al. 2022a) manages to apply diffusion models for object detection, where the bounding boxes of objects are generated from Gaussian noise inputs conditioned on the image features. In this paper, we take the first step in employing diffusion models in video grounding by formulating it as a conditional generative task, where the target span is predicted in a generative manner conditioned on video-sentence multi-modal representations.

Video-Language Transformers

Simultaneously understanding representations from both video and language is the major challenge for video-language models. Inspired by the great success of Transformers (Vaswani et al. 2017) in natural language processing, many studies (Sun et al. 2019; Li et al. 2020; Lei et al. 2021; Tang, Lei, and Bansal 2021; Xu et al. 2021) extend the Transformer-based architecture to video-language tasks, including video captioning (Zhou et al. 2018), video question

answering (Lei et al. 2018) and text-to-video retrieval (Jun et al. 2016). Our proposed DiffusionVG also utilizes the architecture of Transformers and incorporates specialized encoder and decoder to generate the target span through the denoising diffusion process.

Method

Preliminaries

Video Grounding Task Formulation. Given an untrimmed video $\mathbf{V} = \{v_m\}_{m=1}^M$ consisting of M consecutive frames and a sentence query $\mathbf{Q} = \{q_n\}_{n=1}^N$ with N words, a VG model aims to localize the start and end timestamps $\mathbf{z}_0 = (\tau_s, \tau_e)$ of the target moment (termed as target span) in \mathbf{V} that best matches the query \mathbf{Q} , where v_m demotes the m -th frame in \mathbf{V} and q_n demotes the n -th word in \mathbf{Q} . In our setting, VG is framed as a conditional generation task, where the target span is generated through the reverse process of diffusion models. To achieve this, a denoising network θ is adopted to recover the target span \mathbf{z}_0 from the noisy span \mathbf{z}_t , with the video \mathbf{V} and query \mathbf{Q} serving as conditions.

Diffusion Model. Diffusion models (Sohl-Dickstein et al. 2015; Song and Ermon 2019; Ho, Jain, and Abbeel 2020) are a class of likelihood-based generative models consisting of a forward process and a reverse process, both of which can be considered as a Markov chain. Formally, given a data sample \mathbf{z}_0 from distribution $q(\mathbf{z}_0)$ and a predefined noise schedule $\{\beta_1, \dots, \beta_T\}$ for T steps, the forward process transforms \mathbf{z}_0 to the noisy latent sample \mathbf{z}_t for $t \in \{0, 1, \dots, T\}$ by gradually adding Gaussian noise to \mathbf{z}_0 , formulated as:

$$q(\mathbf{z}_t | \mathbf{z}_0) = \mathcal{N}(\mathbf{z}_t; \sqrt{\bar{\alpha}_t} \mathbf{z}_0, (1 - \bar{\alpha}_t) \mathbf{I}), \quad (1)$$

where $\bar{\alpha}_t = \prod_{k=1}^t \alpha_k = \prod_{k=1}^t (1 - \beta_k)$ is commonly pre-calculated for efficient one-step sampling at an arbitrary time step t . In the training stage, a neural network θ is learned to predict \mathbf{z}_0 from \mathbf{z}_t as $\hat{\mathbf{z}}_0 = f_\theta(\mathbf{z}_t, t)$, which can be optimized with a ℓ_2 loss function according to the derivation

Algorithm 1: Training

```

1 repeat
2   Sample a video  $\mathbf{V}$  and a query  $\mathbf{Q}$  with target span  $\mathbf{z}_0$ 
3   Extract video features  $\tilde{\mathbf{F}}^V$  and sentence features  $\tilde{\mathbf{F}}^Q$ 
4    $\mathbf{H} = \text{Encoding}(\tilde{\mathbf{F}}^V, \tilde{\mathbf{F}}^Q)$ 
5    $t \sim \text{Uniform}(\{1, \dots, T\})$ 
6    $\epsilon \sim \mathcal{N}(\mathbf{0}, \mathbf{I})$ 
7    $\mathbf{z}_t = \sqrt{\bar{\alpha}_t} \mathbf{z}_0 + \sqrt{1 - \bar{\alpha}_t} \epsilon$ 
8   Recover  $\mathbf{z}_0$  by computing  $\hat{\mathbf{z}}_0 = f_\theta(\mathbf{z}_t, \mathbf{H}, t)$ 
9   Computing the span loss function for optimization
10 until converged;

```

in (Ho, Jain, and Abbeel 2020):

$$\mathcal{L}_{\text{obj}} = \frac{1}{2} \|\mathbf{f}_\theta(\mathbf{z}_t, t) - \mathbf{z}_0\|^2. \quad (2)$$

During inference, a data sample \mathbf{z}_0 can be derived from a Gaussian noise \mathbf{z}_T with θ in an iterative manner. To speed up the sampling process, our method incorporates the DDIM updating rule presented in (Song, Meng, and Ermon 2020).

DiffusionVG Model

As shown in Fig. 2, our DiffusionVG framework consists of two core components: multi-modal feature encoding and target span generation. In multi-modal feature encoding, we initially employ distinct uni-modal backbones to extract features from both video and sentence inputs. These uni-modal features are subsequently fused in the video-centered multi-modal encoder, resulting in text-enhanced video features. In target span generation, the text-enhanced video features serve as conditions to guide the denoising diffusion process for generating the target span.

Feature Extraction. For video feature extraction, we follow the previous work (Zhang et al. 2020b) and employ a pretrained 3D convolutional network (e.g., C3D (Tran et al. 2015)) to extract video features. Specifically, given an input video consisting of M frames, we identically segment the video into small clips $\{v_i\}_{i=1}^{M/m}$, with each clip comprising m frames. Next, we employ the pretrained 3D convolutional network to extract clip-level features. We perform a fixed-length sampling with an even stride $\frac{M}{m \cdot K}$ to obtain K clip-level features. These fixed-length features are then fed into a fully connected (FC) layer for dimension reduction, resulting in the final video features $\mathbf{F}^V \in \mathbb{R}^{K \times d}$.

For sentence feature extraction, we employ a standard pretrained language model (e.g., DistilBERT (Sanh et al. 2019)) to extract the word-level features from \mathbf{Q} , followed by dimension reduction via an FC layer to match the dimension of video features, resulting in $\mathbf{F}^Q \in \mathbb{R}^{N \times d}$.

Video-centered multi-modal Encoding. To enhance the representations of the target moment in the video, our DiffusionVG employs a video-centered multi-modal encoder that consistently integrates sentence information into the contextualized video features. Generally, our video-centered multi-modal encoder comprises a stack of N_1 post-normalization Transformer encoder layers with modification. Each encoder layer consists of a video self-attention layer, a text-to-video

Algorithm 2: Inference

```

1 Extract video features  $\tilde{\mathbf{F}}^V$  and sentence features  $\tilde{\mathbf{F}}^Q$ 
2  $\mathbf{H} = \text{Encoding}(\tilde{\mathbf{F}}^V, \tilde{\mathbf{F}}^Q)$ 
3  $\mathbf{z}_T \sim \mathcal{N}(\mathbf{0}, \mathbf{I}) \in \mathbb{R}^{N_q \times 2}$ 
4  $s$  is the reversed sampling steps of length  $\tau$  with  $s_\tau = T$ 
5 for  $i = \tau, \dots, 1$  do
6   | Compute  $\hat{\mathbf{z}}_0$  with  $f_\theta(\mathbf{z}_{s_i}, \mathbf{H}, s_i)$ 
7   |  $\mathbf{z}_{s_{i-1}} = \text{ddim\_step}(\mathbf{z}_{s_i}, \hat{\mathbf{z}}_0, s_i, s_{i-1})$ 
8 end
9 Select the final predicted span via voting
10 return final span

```

cross attention layer and a feed-forward (FFN) layer. With the video and sentence features available, we first add a sine positional embedding \mathbf{P}^V to video features and a learnable position embedding \mathbf{P}^Q to sentence features (Vaswani et al. 2017), resulting in $\tilde{\mathbf{F}}^V$ and $\tilde{\mathbf{F}}^Q$, which then serve as inputs to the video-centered multi-modal encoder. Within the video self-attention layer, intra-modal self-attention is performed between clip-level features to derive the contextualized video features. In the text-to-video cross-attention layer, the query for cross-attention is obtained from video features, while key-value pairs are sourced from sentence features. Therefore, only the video features are updated in this layer. Furthermore, a feed-forward network (FFN) is exclusively applied to the video features. The output of the last FFN layer in our video-centered multi-modal encoder yields the text-enhanced video features, denoted as $\mathbf{H} \in \mathbb{R}^{K \times d}$, which serve as conditions to guide the generation of the target span in the subsequent denoising diffusion process.

Span Refining in Decoding. During the target span generation process, DiffusionVG takes N_q Gaussian noise spans as inputs and iteratively refines them through the reverse diffusion process, with conditioning on the text-enhanced video features \mathbf{H} . In order to enhance the refinement within the generation process, we incorporate a span refining decoder that facilitates further refinement of span predictions at each decoding layer. Specifically, each layer of our span refining decoder is composed of a cross-attention and a feed-forward sub-layer, which takes the noisy spans, time step t and the encoded text-enhanced video-centered features \mathbf{H} as inputs. We crop the segments of \mathbf{H} corresponding to the noisy spans \mathbf{z}_t and apply a soft-pooling operation to aggregate the features in each segment as span proposals for decoding. The output of every decoder layer estimates the differences between the input noisy spans and the target span, which are subsequently utilized to update the noisy spans that serve as the inputs of the next decoder layer. Through the updates in the stack of N_2 decoder layers, the output spans from the last decoder layer corresponds to the predicted target spans at time step t . More information and detailed calculations for our span refining decoder can be found in Appendix A.

, as depicted in Fig. 5.

Training Strategy

During training, our DiffusionVG produces the noisy spans by adding Gaussian noise to the ground-truth span and then

Method	Setting	Video Feature	Charades-STA				ActivityNet Captions			
			R@1 IoU=0.3	R@1 IoU=0.5	R@1 IoU=0.7	Video Feature	R@1 IoU=0.3	R@1 IoU=0.5	R@1 IoU=0.7	
CTRL (Gao et al. 2017)	PB	C3D	-	23.63	8.89	C3D	-	29.01	10.34	
QSPN (Xu et al. 2018)	PB	C3D	54.70	35.60	15.80	C3D	45.30	33.26	13.43	
BPNet (Xiao et al. 2022)	PB	C3D	65.48	50.75	31.64	C3D	58.98	42.07	24.69	
2DTAN (Zhang et al. 2020b)	PB	C3D	-	39.81	23.25	C3D	-	44.51	27.38	
SCDM (Yuan et al. 2022)	PB	I3D	-	54.44	33.43	C3D	54.80	36.75	19.86	
CBLN (Liu et al. 2021)	PB	I3D	-	61.13	38.22	C3D	48.12	27.60		
MMN* (Wang et al. 2021)	PB	VGG	-	47.31	27.28	C3D	-	47.26	28.59	
DRN (Zeng et al. 2020)	PF	I3D	-	53.09	31.75	C3D	-	45.45	24.36	
CPNet (Li, Guo, and Wang 2021)	PF	I3D	-	60.27	38.74	C3D	-	40.56	21.63	
CPN (Zhao et al. 2021)	PF	I3D	<u>75.53</u>	59.77	36.67	C3D	<u>62.81</u>	45.10	<u>28.10</u>	
ACRM (Tang et al. 2022)	PF	I3D	<u>73.47</u>	57.53	<u>38.33</u>	C3D	-	31.67	11.25	
VSLNet-L (Zhang et al. 2021a)	PF	I3D	70.46	54.19	35.22	I3D	62.35	43.86	27.51	
DiffusionVG (1-step)	GN	I3D	71.72	59.95	37.32	C3D	61.88	42.54	24.32	
DiffusionVG (5-step)	GN	I3D	76.55	61.78	38.64	C3D	63.03	46.09	26.71	

Table 1: Performance compared with the state-of-the-art methods on Charades-STA and ActivityNet Captions datasets, where **PB** denotes the proposal-based setting, **PF** denotes the proposal-free setting and **GN** denotes our unique generative setting. In order to minimize the influence of randomness, we replicate all DiffusionVG experiments three times and record the average results. (Best results in bold and second in underline, * refers to reproduced results from official implementation.)

learns the reverse process conditioned on the video-sentence representations, as depicted in Algorithm. 1.

Noisy Spans. We introduce Gaussian noises to the ground-truth span to obtain the noisy spans. The schedule of the noises is regulated by the predefined α_t in Eq. 1. In line with (Nichol and Dhariwal 2021), we employ a monotonically decreasing cosine schedule at different time step t . As a data augmentation approach, we replicate the ground-truth span N_d times with various time step t and add independent Gaussian noises to them. Through the utilization of parallel computing, this approach accelerates the convergence of training process. Following (Chen et al. 2022a), we enhance the signal-to-noise ratio (SNR) in the forward diffusion process by multiplying a scaling factor λ to the ground-truth span before injecting noises. This technique has demonstrated promising potential in improving the performance of DiffusionVG when an appropriate λ is utilized.

Loss Function. The output of DiffusionVG is solely comprised of the predicted target spans, each of which is supervised by the same ground-truth span. We apply a combination of a ℓ_1 loss and a generalized IoU (GIoU) (Rezatofighi et al. 2019) loss for optimization, formulated as:

$$\mathcal{L} = \lambda_{\ell_1} \cdot \mathcal{L}_{\ell_1}(\hat{\mathbf{z}}_0, \mathbf{z}_0) + \lambda_{\text{giou}} \cdot \mathcal{L}_{\text{giou}}(\hat{\mathbf{z}}_0, \mathbf{z}_0), \quad (3)$$

where λ_{ℓ_1} and λ_{giou} are the balancing weights of each component. Moreover, auxiliary loss (Carion et al. 2020) is incorporated in every decoder layer to accelerate convergence.

Inference

In inference, our proposed DiffusionVG takes Gaussian noises as inputs and generates the target spans with iterative refinement through the reverse diffusion process, as depicted in Algorithm. 2. The whole generation process is conditioned on the encoded video-sentence representations. It is worth noting that once DiffusionVG finishes training, it becomes flexible to utilize an arbitrary number of sampling steps and queries (noisy spans inputs) in inference, regardless of the configurations in the training stage.

Sampling Process. In each sampling step t , the noisy spans obtained from the previous step (or Gaussian noise inputs)

are fed into the span refining decoder to generate the predictions of the target span. Once the predicted target spans at current step t are acquired, we employ the DDIM (Song, Meng, and Ermon 2020) updating strategy to produce the noisy spans for the next step. The final predicted target spans of DiffusionVG are derived from the last sampling step.

Voting Strategy. Unlike the settings in object detection, our decoder does not estimate the scores of each generated span in the reverse diffusion process, since all queries aim to reconstruct the same target span rather than the set matching problem in (Carion et al. 2020; Chen et al. 2022a). In order to determine the best prediction among all generated spans, we present a voting strategy where all spans participate in a voting process with each other to determine the scores for each candidate. Specifically, we calculate the IoU of each generated span with all other spans and use a sum of these IoUs as its score. The span with the highest score is selected as the final prediction. The validation of the voting strategy can be found in Appendix B.

Experiments

In this section, we provide a comprehensive evaluation of our proposed DiffusionVG and compare it with state-of-the-art methods. We start by introducing the datasets and evaluation metrics, followed by the implementation details. Next, we compare DiffusionVG with existing methods in VG and conduct extensive ablation studies. Finally, we showcase the qualitative results obtained from DiffusionVG.

Datasets and Metrics

To demonstrate the effectiveness of our proposed method, we conduct experiments on two challenging benchmark datasets: Charades-STA (Gao et al. 2017) and ActivityNet Captions (Krishna et al. 2017).

Charades-STA. This dataset includes a total of 6,672 videos depicting daily indoor activities. Each video is annotated with sentence descriptions focusing on specific temporal moments. Specifically, this dataset contains 12,408 (from

Architecture	N_s	N_q	R1@0.3	R1@0.5	R1@0.7
DETR-like	-	1	66.18	51.94	29.01
DETR-like	-	5	66.88	52.45	31.26
DiffusionVG	1	1	73.39	59.39	35.38
DiffusionVG	1	5	75.39	61.27	37.02
DiffusionVG	5	1	74.94	60.60	38.16
DiffusionVG	5	5	76.55	61.78	38.64

Table 2: **Comparison with DETR-like baselines.** N_s denotes the number of sampling steps for DiffusionVG and N_q denotes the number of queries utilized in both models. Experiments are conducted on the Charades-STA dataset.

5,338 videos) moment-sentence pairs for training and 3,720 (from 1,334 videos) moment-sentence pairs for testing.

ActivityNet Captions. This dataset consists of around 20k videos in diverse human activities. Following the settings in previous works (Zhang et al. 2020b, 2021a), we use its original training set for training, val.1 subset for validation and val.2 subset for testing, which have 37,417, 17,505 and 17,031 moment-sentence pairs, respectively.

Evaluation Metrics. We follow (Gao et al. 2017) and evaluate DiffusionVG with the commonly used “Rank@ n , IoU= m ” (Rn@m) metric. The Rn@m metric calculates the percentage of the sentence queries that have at least one predicted moment whose temporal Intersection over Union (IoU) is larger than the threshold m with the ground-truth moment among the top- n predicted moments. In our experiments, we employ the most commonly adopted R1@0.3, R1@0.5 and R1@0.7 metrics for both Charades-STA and ActivityNet Captions datasets.

Implementation Details

We train DiffusionVG using AdamW (Loshchilov and Hutter 2017) optimizer with a learning rate of $1e^{-4}$ and a weight decay of $1e^{-4}$. The batch size is set to 64 on both Charades-STA and ActivityNet Captions datasets. For a fair comparison with existing VG methods, we extract video features using I3D (Carreira and Zisserman 2017) for Charades-STA and C3D (Tran et al. 2015) for ActivityNet Captions. For both datasets, we set the length of the video features K to 64. We extract the sentence features with a pretrained DistilBERT-base model (Sanh et al. 2019) from the *Transformers* library (Wolf et al. 2020). For the diffusion strategy, we adopt a monotonically decreasing cosine schedule to control the noises and set the diffusion steps as $T = 1000$. We empirically set the balancing weights in Eq. 3 as $\lambda_{\ell 1} = 1.5$ and $\lambda_{giou} = 1$, while the scaling factor λ is set to 2.

Comparison with State-of-the-arts

To validate the effectiveness of our proposed DiffusionVG model, we compare it with state-of-the-art VG methods on both Charades-STA and ActivityNet Captions datasets in Tab. 1. The compared methods can be divided into two groups: (1) **Proposal-based Methods:** CTRL (Gao et al. 2017), QSPN (Xu et al. 2018), BPNet (Xiao et al. 2022), 2DTAN (Zhang et al. 2020b), SCDM (Yuan et al. 2022), CBLN (Liu et al. 2021) and MMN (Wang et al.

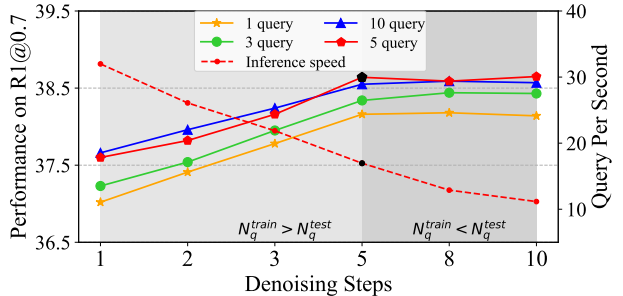


Figure 3: Evaluating the impact of **sampling steps** and **number of queries** on model performance and inference speed (5 queries). All experiments are conducted on Charades-STA test set. Black markers denote the default setting.

2021). These methods employ a propose-and-rank pipeline, wherein a set of moment proposals are pre-sampled from the input video. Subsequently, these proposals are matched with the sentence query to identify the optimal moment by means of cross-modal alignment. (2) **Proposal-free Methods:** DRN (Zeng et al. 2020), CPNet (Li, Guo, and Wang 2021), CPN (Zhao et al. 2021), ACRM (Tang et al. 2022) and VSLNet-L (Zhang et al. 2021a). These methods perform direct regression of the start and end timestamps from each frame or predict the probabilities for each frame to determine whether it serves as the start or end frame.

Main Results. Notably, our proposed DiffusionVG demonstrates competitive performance on both benchmarks and achieves new state-of-the-art on the Charades-STA dataset. Without relying on meticulously crafted model architectures or specifically tailored learning strategies, our DiffusionVG surpasses all its discriminative learning-based counterparts like proposal-based SCDM and proposal-free VSLNet-L. This demonstrates the potential of the diffusion model in tackling the VG task, as its iterative framework allows for continuous refinement of the target moment prediction.

Comparison with DETR-like Baselines. There have been some studies employing Transformer-based models for the VG task (Woo et al. 2022; Cao et al. 2021). However, due to the adoption of distinct video features and issue of irreproducibility in these works, we do not compare our method with them in this paper. To demonstrate the superiority of DiffusionVG over Transformer-based baselines, we compare it with DETR-like (Carion et al. 2020) multi-modal Transformer models under the same parameter settings.

As indicated in Tab. 2, our DiffusionVG outperforms the DETR-like baselines across all evaluation metrics in the VG task, utilizing the same parameter settings. It is worth noting that even without employing multiple sampling steps, our DiffusionVG significantly outperforms DETR-like baselines by a large margin (8.82% in R1@0.5 and 5.76% in R1@0.7) while employing the same number of 5 queries. We posit that this may due to the dilemma of defining the optimal learning objective for all learnable queries in DETR-like models. Specifically, when employing just one query, it may conform to a particular pattern in aligning video and sentence features, resulting in limited sensitivity to the rich representations of both videos and sentences. However, uti-

VcE	SRD	R1@0.3	R1@0.5	R1@0.7
✓	✓	73.04	59.22	35.29
		74.74	60.67	36.77
✓	✓	74.92	61.07	37.58
		76.55	61.96	38.42

Table 3: Ablation study on our **video-centered encoder** (VcE) and **span refining decoder** (SRD).

lizing multiple queries presents the challenge of determining an appropriate learning objective for all predictions, since the rest predictions apart from the best-matched one may be considered as “sub-optimal” answers without being strictly incorrect. In contrast, the learning objective for all predictions in DiffusionVG is the recovery of a single ground-truth span, thus allowing flexibility in the number of queries. The utilization of multiple queries during the training stage can be considered a form of data augmentation. Thanks to the iterative refinement through the reverse diffusion process and the voting strategy, our DiffusionVG can precisely obtain the target span candidates and accurately select the best one.

Ablation Study

In this section, we conduct comprehensive ablation experiments on the Charades-STA dataset to study DiffusionVG in detail. We first evaluate the impact of different sampling steps and number of queries in Fig. 3. Furthermore, we study the effectiveness of our proposed video-centered encoder and span-refining decoder in Tab. 3.

Sampling Steps. Notably, as the number of sampling steps increases, the model achieves gradual performance improvement while sacrificing inference speed. In the case of utilizing 5 queries as an example, when we employ only one step to generate the target span from Gaussian noise inputs, the model witnesses a substantial decline in performance (1.83%, 1.04% in R1@0.5, R1@0.7). This observation demonstrates the effectiveness of the iterative refining process in DiffusionVG, which facilitates the recovery of the target span through a step-by-step approach.

Number of Queries. Intuitively, a single query (input noisy span) suffices for recovering the target span in DiffusionVG. However, as shown in Fig. 3, the model performance can be enhanced as the number of queries increases in a certain range (from 1 to 5). We hypothesize that utilizing a limited number of queries contributes to the rising uncertainty through the generation process. Moreover, beyond a certain threshold, increasing the number of queries can have adverse effects on model performance (from 5 to 10). This may be attributed to the concurrent rise in low-quality predictions, leading to disturbances in the voting process for determining the best prediction.

Encoder and Decoder Designing. To demonstrate the effectiveness of our video-centered encoder and span refining decoder in DiffusionVG, we compare them with a standard multi-modal Transformer encoder-decoder architecture. In the standard Transformer, the encoder facilitates interaction between the multi-modal information, while the decoder ensures continuous attention of queries to the encoded

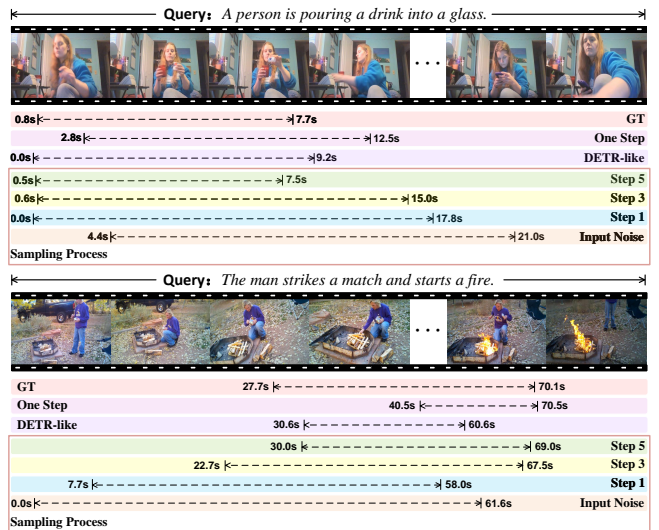


Figure 4: Visualized examples of the proposed DiffusionVG in the VG task. (top: Charades-STA, bottom: ActivityNet Captions, only one query is adopted.)

multi-modal features. As shown in Tab. 3, both our video-centered encoder and span refining decoder contribute to the improved performance of DiffusionVG, comparing with the standard counterparts. Furthermore, the improvements brought by both modules are compatible with each other and further enhance the overall performance.

Visualization

In Fig. 4, we visualize some predictions from our DiffusionVG with 5 sampling steps and the DETR-like baselines on both Charades-STA and ActivityNet Captions datasets. Additionally, we present the corresponding results from the one-step generation approach in DiffusionVG to highlight the effectiveness of the iterative refining process in the multi-step generation approach. It can be observed that both the DETR-like baselines and the one-step DiffusionVG model can understand the semantics of both video and sentence contents and localize a video segment that, to some extent, relates to the sentence query. However, it is noteworthy that their predicted moments suffer significant deviations from the ground truth. In contrast, our multi-step generation strategy in DiffusionVG can perform iterative refinement on the predictions by mitigating the disparities between the noisy spans and the target span, which demonstrates the best grounding results compared to the DETR-like baselines and the one-step approach.

Conclusion

In this paper, we propose DiffusionVG, a pioneering approach that addresses the video grounding task from the perspective of conditional generation. By employing a multi-step generation process through the denoising diffusion process in DiffusionVG, the predicted spans undergo iterative refinement starting from Gaussian noise inputs. Extensive experiments on mainstream benchmarks have demonstrated its superiority over existing state-of-the-art methods in VG.

References

Amit, T.; Shaharbany, T.; Nachmani, E.; and Wolf, L. 2021. Segdiff: Image segmentation with diffusion probabilistic models. *arXiv preprint arXiv:2112.00390*.

Austin, J.; Johnson, D.; Ho, J.; Tarlow, D.; and Berg, R. 2021. Structured Denoising Diffusion Models in Discrete State-Spaces. *arXiv: Learning,arXiv: Learning*.

Baranchuk, D.; Rubachev, I.; Voynov, A.; Khrulkov, V.; and Babenko, A. 2021. Label-efficient semantic segmentation with diffusion models. *arXiv preprint arXiv:2112.03126*.

Cao, M.; Chen, L.; Shou, M.; Zhang, C.; and Zou, Y. 2021. On Pursuit of Designing Multi-modal Transformer for Video Grounding. *Empirical Methods in Natural Language Processing,Empirical Methods in Natural Language Processing*.

Carion, N.; Massa, F.; Synnaeve, G.; Usunier, N.; Kirillov, A.; and Zagoruyko, S. 2020. *End-to-End Object Detection with Transformers*, 213–229.

Carreira, J.; and Zisserman, A. 2017. Quo Vadis, Action Recognition? A New Model and the Kinetics Dataset. In *2017 IEEE Conference on Computer Vision and Pattern Recognition (CVPR)*.

Chen, J.; Chen, X.; Ma, L.; Jie, Z.; and Chua, T.-S. 2018. Temporally Grounding Natural Sentence in Video. In *Proceedings of the 2018 Conference on Empirical Methods in Natural Language Processing*.

Chen, L.; Lu, C.; Tang, S.; Xiao, J.; Zhang, D.; Tan, C.; and Li, X. 2020a. Rethinking the Bottom-Up Framework for Query-Based Video Localization. *Proceedings of the AAAI Conference on Artificial Intelligence*, 10551–10558.

Chen, S.; Jiang, W.; Liu, W.; and Jiang, Y.-G. 2020b. *Learning Modality Interaction for Temporal Sentence Localization and Event Captioning in Videos*, 333–351.

Chen, S.; and Jiang, Y.-G. 2019. Semantic Proposal for Activity Localization in Videos via Sentence Query. *Proceedings of the AAAI Conference on Artificial Intelligence*, 8199–8206.

Chen, S.; and Jiang, Y.-G. 2020. *Hierarchical Visual-Textual Graph for Temporal Activity Localization via Language*, 601–618.

Chen, S.; Sun, P.; Song, Y.; and Luo, P. 2022a. Diffusion-det: Diffusion model for object detection. *arXiv preprint arXiv:2211.09788*.

Chen, T.; Li, L.; Saxena, S.; Hinton, G.; and Fleet, D. 2022b. A Generalist Framework for Panoptic Segmentation of Images and Videos. *arXiv preprint arXiv:2210.06366*.

Dhariwal, P.; and Nichol, A. 2021. Diffusion Models Beat GANs on Image Synthesis. *arXiv: Learning,arXiv: Learning*.

Fan, W.-C.; Chen, Y.-C.; Chen, D.; Cheng, Y.; Yuan, L.; and Wang, Y.-C. F. 2023. Frido: Feature pyramid diffusion for complex scene image synthesis. *Proceedings of the AAAI Conference on Artificial Intelligence*, 37(1): 579–587.

Fu, T.-J.; Wang, X. E.; Grafton, S. T.; Eckstein, M. P.; and Wang, W. Y. 2022. M3L: Language-based video editing via multi-modal multi-level transformers. In *Proceedings of the IEEE/CVF Conference on Computer Vision and Pattern Recognition*, 10513–10522.

Gao, J.; Sun, C.; Yang, Z.; and Nevatia, R. 2017. TALL: Temporal Activity Localization via Language Query. In *2017 IEEE International Conference on Computer Vision (ICCV)*.

Ge, R.; Gao, J.; Chen, K.; and Nevatia, R. 2018. MAC: Mining Activity Concepts for Language-based Temporal Localization. *Cornell University - arXiv,Cornell University - arXiv*.

Gong, S.; Li, M.; Feng, J.; Wu, Z.; and Kong, L. 2022. DiffuSeq: Sequence to Sequence Text Generation with Diffusion Models. *arXiv preprint arXiv:2210.08933*.

Gu, S.; Chen, D.; Bao, J.; Wen, F.; Zhang, B.; Chen, D.; Yuan, L.; and Guo, B. 2022. Vector Quantized Diffusion Model for Text-to-Image Synthesis. In *2022 IEEE/CVF Conference on Computer Vision and Pattern Recognition (CVPR)*.

Harvey, W.; Naderiparizi, S.; Masrani, V.; Weilbach, C.; and Wood, F. 2022. Flexible Diffusion Modeling of Long Videos. *Advances in Neural Information Processing Systems*, 35: 27953–27965.

Hendricks, L. A.; Wang, O.; Shechtman, E.; Sivic, J.; Darrell, T.; and Russell, B. 2017. Localizing Moments in Video with Natural Language. In *2017 IEEE International Conference on Computer Vision (ICCV)*.

Ho, J.; Jain, A.; and Abbeel, P. 2020. Denoising Diffusion Probabilistic Models. *Neural Information Processing Systems,Neural Information Processing Systems*.

Jun, X.; Tao, M.; Ting, Y.; and Yong, R. 2016. MSR-VTT: A Large Video Description Dataset for Bridging Video and Language. *IEEE Conference Proceedings,IEEE Conference Proceedings*.

Krishna, R.; Hata, K.; Ren, F.; Fei-Fei, L.; and Carlos Niebles, J. 2017. Dense-captioning events in videos. In *Proceedings of the IEEE international conference on computer vision*, 706–715.

Lei, J.; Li, L.; Zhou, L.; Gan, Z.; Berg, T. L.; Bansal, M.; and Liu, J. 2021. Less is more: Clipbert for video-and-language learning via sparse sampling. In *Proceedings of the IEEE/CVF conference on computer vision and pattern recognition*, 7331–7341.

Lei, J.; Yu, L.; Bansal, M.; and Berg, T. 2018. TVQA: Localized, Compositional Video Question Answering. In *Proceedings of the 2018 Conference on Empirical Methods in Natural Language Processing*.

Li, K.; Guo, D.; and Wang, M. 2021. Proposal-Free Video Grounding with Contextual Pyramid Network. *Proceedings of the ... AAAI Conference on Artificial Intelligence,Proceedings of the ... AAAI Conference on Artificial Intelligence*.

Li, L.; Chen, Y.-C.; Cheng, Y.; Gan, Z.; Yu, L.; and Liu, J. 2020. HERO: Hierarchical Encoder for Video+Language Omni-representation Pre-training. In *Proceedings of the 2020 Conference on Empirical Methods in Natural Language Processing (EMNLP)*.

Li, X.; Thickstun, J.; Gulrajani, I.; Liang, P. S.; and Hashimoto, T. B. 2022. Diffusion-lm improves controllable text generation. *Advances in Neural Information Processing Systems*, 35: 4328–4343.

Liu, D.; Qu, X.; Dong, J.; Zhou, P.; Cheng, Y.; Wei, W.; Xu, Z.; and Xie, Y. 2021. Context-aware Biaffine Localizing Network for Temporal Sentence Grounding. *Cornell University - arXiv, Cornell University - arXiv*.

Liu, D.; Qu, X.; Liu, X.-Y.; Dong, J.; Zhou, P.; and Xu, Z. 2020. Jointly Cross- and Self-Modal Graph Attention Network for Query-Based Moment Localization. *Cornell University - arXiv, Cornell University - arXiv*.

Liu, M.; Wang, X.; Nie, L.; Tian, Q.; Chen, B.; and Chua, T.-S. 2018. Cross-modal Moment Localization in Videos. In *Proceedings of the 26th ACM international conference on Multimedia*.

Loshchilov, I.; and Hutter, F. 2017. Decoupled Weight Decay Regularization. *Learning, Learning*.

Mun, J.; Cho, M.; and Han, B. 2020. Local-Global Video-Text Interactions for Temporal Grounding. In *2020 IEEE/CVF Conference on Computer Vision and Pattern Recognition (CVPR)*.

Nan, G.; Qiao, R.; Xiao, Y.; Liu, J.; Leng, S.; Zhang, H.; and Lu, W. 2021. Interventional Video Grounding with Dual Contrastive Learning. In *2021 IEEE/CVF Conference on Computer Vision and Pattern Recognition (CVPR)*.

Nichol, A.; and Dhariwal, P. 2021. Improved Denoising Diffusion Probabilistic Models. *Cornell University - arXiv, Cornell University - arXiv*.

Nichol, A.; Dhariwal, P.; Ramesh, A.; Shyam, P.; Mishkin, P.; McGrew, B.; Sutskever, I.; and Chen, M. 2021. GLIDE: Towards Photorealistic Image Generation and Editing with Text-Guided Diffusion Models. *arXiv preprint arXiv:2112.10741*.

Qu, X.; Tang, P.; Zou, Z.; Cheng, Y.; Dong, J.; Zhou, P.; and Xu, Z. 2020. Fine-grained Iterative Attention Network for Temporal Language Localization in Videos. In *Proceedings of the 28th ACM International Conference on Multimedia*.

Rezatofighi, H.; Tsoi, N.; Gwak, J.; Sadeghian, A.; Reid, I.; and Savarese, S. 2019. Generalized Intersection over Union: A Metric and A Loss for Bounding Box Regression. In *2019 IEEE/CVF Conference on Computer Vision and Pattern Recognition (CVPR)*.

Rombach, R.; Blattmann, A.; Lorenz, D.; Esser, P.; and Ommer, B. 2022. High-Resolution Image Synthesis with Latent Diffusion Models. In *2022 IEEE/CVF Conference on Computer Vision and Pattern Recognition (CVPR)*.

Saharia, C.; Chan, W.; Saxena, S.; Li, L.; Whang, J.; Denton, E. L.; Ghasemipour, K.; Gontijo Lopes, R.; Karagol Ayan, B.; Salimans, T.; et al. 2022. Photorealistic text-to-image diffusion models with deep language understanding. *Advances in Neural Information Processing Systems*, 35: 36479–36494.

Sanh, V.; Debut, L.; Chaumond, J.; and Wolf, T. 2019. DistilBERT, a distilled version of BERT: smaller, faster, cheaper and lighter. *arXiv preprint arXiv:1910.01108*.

Shen, Y.; Song, K.; Tan, X.; Li, D.; Lu, W.; and Zhuang, Y. 2023. DiffusionNER: Boundary Diffusion for Named Entity Recognition. *arXiv preprint arXiv:2305.13298*.

Sohl-Dickstein, J.; Weiss, E.; Maheswaranathan, N.; and Ganguli, S. 2015. Deep Unsupervised Learning using Nonequilibrium Thermodynamics. *arXiv: Learning, arXiv: Learning*.

Song, J.; Meng, C.; and Ermon, S. 2020. Denoising Diffusion Implicit Models. *arXiv: Learning, arXiv: Learning*.

Song, Y.; and Ermon, S. 2019. Generative Modeling by Estimating Gradients of the Data Distribution. *Cornell University - arXiv, Cornell University - arXiv*.

Song, Y.; Sohl-Dickstein, J.; Kingma, D.; Kumar, A.; Ermon, S.; and Poole, B. 2021. Score-Based Generative Modeling through Stochastic Differential Equations. *International Conference on Learning Representations, International Conference on Learning Representations*.

Strudel, R.; Tallec, C.; Altché, F.; Du, Y.; Ganin, Y.; Mensch, A.; Grathwohl, W.; Savinov, N.; Dieleman, S.; Sifre, L.; et al. 2022. Self-conditioned embedding diffusion for text generation. *arXiv preprint arXiv:2211.04236*.

Sun, C.; Myers, A.; Vondrick, C.; Murphy, K.; and Schmid, C. 2019. VideoBERT: A Joint Model for Video and Language Representation Learning. In *2019 IEEE/CVF International Conference on Computer Vision (ICCV)*.

Tang, H.; Zhu, J.; Liu, M.; Gao, Z.; and Cheng, Z. 2022. Frame-wise Cross-modal Matching for Video Moment Retrieval. *IEEE Transactions on Multimedia*, 1338–1349.

Tang, Z.; Lei, J.; and Bansal, M. 2021. Decembert: Learning from noisy instructional videos via dense captions and entropy minimization. In *Proceedings of the 2021 Conference of the North American Chapter of the Association for Computational Linguistics: Human Language Technologies*, 2415–2426.

Tran, D.; Bourdev, L.; Fergus, R.; Torresani, L.; and Paluri, M. 2015. Learning Spatiotemporal Features with 3D Convolutional Networks. In *2015 IEEE International Conference on Computer Vision (ICCV)*.

Vaswani, A.; Shazeer, N.; Parmar, N.; Uszkoreit, J.; Jones, L.; Gomez, A.; Kaiser, L.; and Polosukhin, I. 2017. Attention is All you Need. *Neural Information Processing Systems, Neural Information Processing Systems*.

Wang, H.; Zha, Z.-J.; Chen, X.; Xiong, Z.; and Luo, J. 2020. Dual Path Interaction Network for Video Moment Localization. In *Proceedings of the 28th ACM International Conference on Multimedia*.

Wang, J.; Ma, L.; and Jiang, W. 2019. Temporally Grounding Language Queries in Videos by Contextual Boundary-aware Prediction. *Cornell University - arXiv, Cornell University - arXiv*.

Wang, J.; Ma, L.; and Jiang, W. 2020. Temporally Grounding Language Queries in Videos by Contextual Boundary-Aware Prediction. *Proceedings of the AAAI Conference on Artificial Intelligence*, 34(07): 12168–12175.

Wang, Z.; Wang, L.; Wu, T.; Li, T.; and Wu, G. 2021. Negative Sample Matters: A Renaissance of Metric Learning for Temporal Grounding. *Proceedings of the ... AAAI Conference on Artificial Intelligence, Proceedings of the ... AAAI Conference on Artificial Intelligence*.

Wolf, T.; Debut, L.; Sanh, V.; Chaumond, J.; Delangue, C.; Moi, A.; Cistac, P.; Ma, C.; Jernite, Y.; Plu, J.; Xu, C.; Scao, T.; Gugger, S.; Drame, M.; Lhoest, Q.; and Rush, A. 2020. Transformers: State-of-the-Art Natural Language Processing. *Empirical Methods in Natural Language Processing, Empirical Methods in Natural Language Processing*.

Wolleb, J.; Sandkühler, R.; Bieder, F.; Valmaggia, P.; and Cattin, P. C. 2022. Diffusion models for implicit image segmentation ensembles. In *International Conference on Medical Imaging with Deep Learning*, 1336–1348. PMLR.

Woo, S.; Park, J.; Koo, I.; Lee, S.; Jeong, M.; and Kim, C. 2022. Explore and match: End-to-end video grounding with transformer. *arXiv preprint arXiv:2201.10168*, 4(5).

Xiao, S.; Chen, L.; Zhang, S.; Ji, W.; Shao, J.; Ye, L.; and Xiao, J. 2022. Boundary Proposal Network for Two-stage Natural Language Video Localization. *Proceedings of the AAAI Conference on Artificial Intelligence*, 2986–2994.

Xu, H.; Ghosh, G.; Huang, P.-Y.; Arora, P.; Aminzadeh, M.; Feichtenhofer, C.; Metze, F.; and Zettlemoyer, L. 2021. Vlm: Task-agnostic video-language model pre-training for video understanding. *arXiv preprint arXiv:2105.09996*.

Xu, H.; He, K.; Plummer, B.; Sigal, L.; Sclaroff, S.; and Saenko, K. 2018. Multilevel Language and Vision Integration for Text-to-Clip Retrieval. *arXiv: Computer Vision and Pattern Recognition, arXiv: Computer Vision and Pattern Recognition*.

Yang, R.; Srivastava, P.; and Mandt, S. 2022. Diffusion Probabilistic Modeling for Video Generation. *arXiv preprint arXiv:2203.09481*.

Ye, Y.; Zhao, Z.; Li, Y.; Chen, L.; Xiao, J.; and Zhuang, Y. 2017. Video Question Answering via Attribute-Augmented Attention Network Learning. In *Proceedings of the 40th International ACM SIGIR Conference on Research and Development in Information Retrieval*.

Yuan, Y.; Ma, L.; Wang, J.; Liu, W.; and Zhu, W. 2022. Semantic Conditioned Dynamic Modulation for Temporal Sentence Grounding in Videos. *IEEE Transactions on Pattern Analysis and Machine Intelligence, IEEE Transactions on Pattern Analysis and Machine Intelligence*.

Yuan, Y.; Mei, T.; and Zhu, W. 2019. To Find Where You Talk: Temporal Sentence Localization in Video with Attention Based Location Regression. *Proceedings of the AAAI Conference on Artificial Intelligence*, 9159–9166.

Zeng, R.; Xu, H.; Huang, W.; Chen, P.; Tan, M.; and Gan, C. 2020. Dense Regression Network for Video Grounding. *arXiv: Computer Vision and Pattern Recognition, arXiv: Computer Vision and Pattern Recognition*.

Zhang, H.; Sun, A.; Jing, W.; Zhen, L.; Zhou, J. T.; and Goh, R. S. M. 2021a. Natural Language Video Localization: A Revisit in Span-based Question Answering Framework. *IEEE Transactions on Pattern Analysis and Machine Intelligence*, 1–1.

Zhang, H.; Sun, A.; Jing, W.; and Zhou, J. T. 2020a. Span-based Localizing Network for Natural Language Video Localization. In *Proceedings of the 58th Annual Meeting of the Association for Computational Linguistics*.

Zhang, H.; Sun, A.; Jing, W.; and Zhou, J. T. 2022. The elements of temporal sentence grounding in videos: A survey and future directions. *arXiv preprint arXiv:2201.08071*, 1(2).

Zhang, L.; and Agrawala, M. 2023. Adding conditional control to text-to-image diffusion models. *arXiv preprint arXiv:2302.05543*.

Zhang, M.; Yang, Y.; Chen, X.; Ji, Y.; Xu, X.; Li, J.; and Shen, H. T. 2021b. Multi-stage Aggregated Transformer Network for Temporal Language Localization in Videos. In *2021 IEEE/CVF Conference on Computer Vision and Pattern Recognition (CVPR)*.

Zhang, S.; Peng, H.; Fu, J.; and Luo, J. 2020b. Learning 2d temporal adjacent networks for moment localization with natural language. In *Proceedings of the AAAI Conference on Artificial Intelligence*, volume 34, 12870–12877.

Zhang, Z.; Lin, Z.; Zhao, Z.; and Xiao, Z. 2019. Cross-Modal Interaction Networks for Query-Based Moment Retrieval in Videos. In *Proceedings of the 42nd International ACM SIGIR Conference on Research and Development in Information Retrieval*.

Zhao, Y.; Zhao, Z.; Zhang, Z.; and Lin, Z. 2021. Cascaded Prediction Network via Segment Tree for Temporal Video Grounding. In *2021 IEEE/CVF Conference on Computer Vision and Pattern Recognition (CVPR)*.

Zhou, L.; Zhou, Y.; Corso, J. J.; Socher, R.; and Xiong, C. 2018. End-to-End Dense Video Captioning with Masked Transformer. In *2018 IEEE/CVF Conference on Computer Vision and Pattern Recognition*.

Appendix

A. Decoder in Details

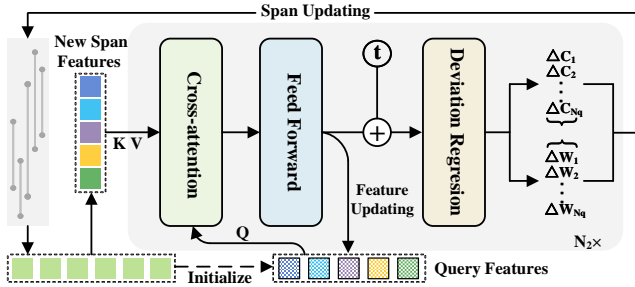


Figure 5: Illustration of the span refining decoder. (Span location embedding is not illustrated.)

In this section, we provide a detailed introduction to our proposed span refining decoder in DiffusionVG. As illustrated in Fig. 5, our span refining decoder takes N_q noisy spans (or Gaussian noises) as inputs and generates the predicted target spans at time step t , with conditioning on the text-enhanced video features \mathbf{H} .

Each layer in our span refining decoder consists of a cross-attention and an FFN sub-layers. We begin with obtaining the span features in decoding stages (similar to the learnable queries in DETR (Carion et al. 2020)), in other words, how to align a noisy span with the encoded multi-modal features. First of all, we crop the feature segment of \mathbf{H} that corresponds to the i -th noisy span \mathbf{z}_t^i . Considering the varying lengths of feature segments within each input noisy span, we apply a soft-pooling operation to aggregate the features in each segment. Specifically, supposing the length of a feature segment for a noisy span \mathbf{z}_t^i is n_t^i , we compute the weights of these n_t^i clip-level features in the segment using a fully connected (FC) layer \mathbf{W}_F followed by a softmax operation. By performing a weighted sum of these clip-level features, we obtain the initial span features of each input noisy span. To incorporate location information into the initial span features, we apply an FC layer \mathbf{W}_E to project \mathbf{z}_t^i onto the dimension of corresponding features as the location embedding (Note that we do not visualize the location embedding in Fig. 5). This location embedding is then added to the initial span features, providing the final span features $\bar{\mathbf{F}}_{\mathbf{z}_t^i}$ for the input noisy span \mathbf{z}_t^i . The entire process can be formulated as follows:

$$\text{Emd}_{\mathbf{z}_t^i} = \mathbf{W}_E(\mathbf{z}_t^i), \quad (4)$$

$$\mathbf{F}_{\mathbf{z}_t^i} = \text{crop}(\mathbf{H}, \mathbf{z}_t^i), \quad (5)$$

$$\mathbf{w}_t^i = \text{softmax}(\mathbf{W}_F(\mathbf{F}_{\mathbf{z}_t^i})), \quad (6)$$

$$\bar{\mathbf{F}}_{\mathbf{z}_t^i} = \sum_{k=1}^{n_t^i} \mathbf{F}_{\mathbf{z}_t^i}[k] \cdot \mathbf{w}_t^i[k] + \text{Emd}_{\mathbf{z}_t^i}. \quad (7)$$

The span features obtained from the input noisy spans \mathbf{z}_t (from last DDIM step or Gaussian noise inputs) are designated as **query features**. In every decoder layer, we update the query features through a cross-attention with the

new span features obtained from new noisy spans updated in the previous decoder layer, as illustrated in the cross-attention operation in Fig. 5. The process of acquiring the new span features from the new noisy spans is analogous to the derivation of the query features from the input noisy spans. Notably, in the first decoder layer where the updated noisy spans are not available, we replace the cross-attention with a self-attention layer for updating the initial query features. Subsequently, the query features are further updated using an additive feed-forward layer, similar to the standard Transformer decoder layer. The time step t is projected into a time embedding through a sine positional embedding (Vaswani et al. 2017) followed with a linear layer and added to the query features. In order to assess the deviation between current noisy spans and the target span, a linear layer is employed to estimate their differences in both centers and widths, which are subsequently utilized to update the noisy spans. Finally, the updated spans from the last decoder layer serve as predictions for the target span at time step t . During training, we directly optimize DiffusionVG by computing the loss function in Eq.3 with the predicted target spans. In inference, we employ the DDIM updating rule to derive $\mathbf{z}_{t-\tau}$ that serves as the inputs of the next denoising step, where τ is the sampling stride.

B. More Ablation Study

In this section, we provide additional ablation studies to further analyze each component in our DiffusionVG. This includes the effects of the **signal scaling** factor λ , the impact of sampling steps and number of queries on **inference speed**, the influence of various **span representations** in decoder, the **stability** and **compatibility** of our DiffusionVG and the evaluation of the **voting strategy**.

Signal Scaling. In Tab. 4, we study the impact of different signal scaling factors that control the signal-to-noise ratios (SNR) of the forward diffusion process. Unexpectedly, our model exhibits apparent sensitivity to the SNR, resulting in significant performance fluctuations with varying scaling factors. Nevertheless, we argue that the choice of the best scaling factor heavily relies on the specific task. For instance, most image generation tasks (Ho, Jain, and Abbeel 2020; Dhariwal and Nichol 2021) prefer the value of 1.0, while it is 0.1 for panoptic segmentation (Chen et al. 2022b) and 2.0 for object detection (Chen et al. 2022a). In line with the latter, our DiffusionVG showcases the best performance with the scaling factor of 2.0.

Scaling	R1@0.3	R1@0.5	R1@0.7
0.5	75.02	61.03	37.35
1.0	73.43	58.72	34.72
2.0	76.55	61.96	38.42
3.0	73.39	59.39	35.38

Table 4: **Signal scaling factor.** Impact of different signal-to-noise ratios on model performance.

Balancing performance and speed. As depicted in Fig.6,

utilizing more sampling steps and number of queries both result in a compromise on the inference speed. Additionally, increasing the number of queries from 1 to 5 only slightly compromises the inference speed compared to the effect of increasing sampling steps. This discrepancy stems from the sequential execution inherent in the diffusion sampling process, while the utilization of multiple queries capitalizes on parallel computing, resulting in enhanced efficiency. Considering the trade-off between achieving better performance while maintaining efficiency, we set both the sampling steps and number of queries to 5 as default values in all experiments.

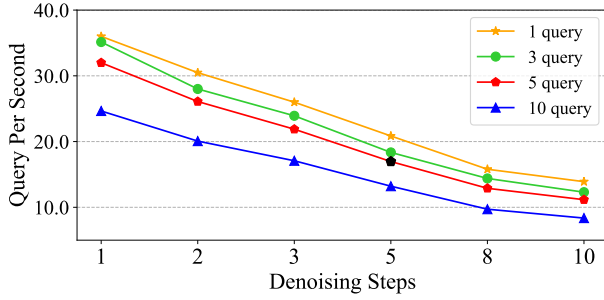


Figure 6: Impact of **sampling steps** and **number of queries** on inference speed. All experiments are conducted on the test set of Charades-STA. (Default in black marker)

Span Representations. In this section, we explore multiple approaches to represent the noisy spans (i.e., the way to align the noisy spans with the encoded multi-modal features \mathbf{H}) in our span refining decoder, including: **(1. feature)** We directly utilize the weighted sum of the features in the segment corresponding to the noisy span; **(2. cat-fn)** We first concatenate the weighted sum of segment features with the span location embedding, then apply an FC layer to project the concatenated features to the dimension of \mathbf{H} for decoding; **(3. add)** The default setting in DiffusionVG, which adds the span location embedding to the weighted sum of segment features. As shown in Tab.5, it can be concluded that simply adding the location embedding to the segment features yields the optimal span representations in our span refining decoder. The reason for why the **add** operation outperforms **cat-fn** may stem from the adverse effects of including an extra FC layer on the structure of the encoded multi-modal features. The comparison between the **add** operation and the **feature** approach highlights the importance of incorporating the span location information.

Scaling	R1@0.3	R1@0.5	R1@0.7
feature	76.44	60.37	36.97
cat-fn	75.48	61.05	37.18
add	76.55	61.96	38.42

Table 5: **Span proposal representations.** Impact of the representations of the noisy spans in our span refining decoder.

Stability and Compatibility. Given that DiffusionVG generates predicted target spans from Gaussian noise inputs in inference and adds sampled noises to the ground-truth span during training, it is worth exploring whether its performance heavily depends on the sampled noises, namely, the random seeds. To demonstrate its stability under different random seeds, we repeat the training process of our DiffusionVG on Charades-STA (Gao et al. 2017) dataset 10 times with distinct random seeds. We showcase all the validation results on R1@0.7 through the training process in Fig. 7. Specifically, the best result and the worst result among the 10 runs are 37.77 and 38.98 in R1@0.7, respectively, while the standard deviation for all runs remains low at 0.44.

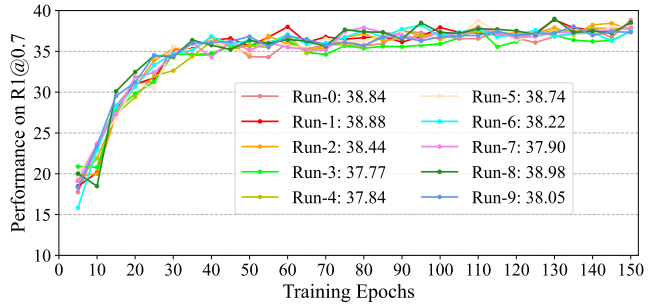


Figure 7: **Stability.** All 10 runs are conducted on Charades-STA dataset. This result demonstrates the stability of DiffusionVG under different random seeds.

To study the compatibility between varying numbers of queries used during training and inference in DiffusionVG, we perform experiments utilizing 1, 5, and 10 queries during training, and evaluate each of these models with 1, 5, and 10 queries in inference. The results are summarized in Tab. 6. Notably, regardless of the number of queries employed during training, a consistent performance improvement is observed across all models as the evaluation queries increases from 1 to 5. However, as the number of queries in evaluation exceeds 5, the performance either experiences a slight decline or remains static. Since the effects of the number of evaluation queries are independent of the number of queries used in training, we can conclude that different query quantities employed in training and inference are mutually compatible. The sole influence of the number of training queries on model performance emerges when training queries are insufficient (first line in Tab. 6), leading to limited data augmentation and hindered convergence for the model.

Train \ Test	1-query	5-query	10-query
1-query	36.72	37.24	37.20
5-query	37.32	38.64	38.55
10-query	37.53	38.47	38.56

Table 6: **Compatibility.** Ablation study on the compatibility between the varying numbers of queries utilized in training and inference stages in DiffusionVG.

Voting Strategy. To validate the effectiveness of our voting strategy, we employ a counterpart mechanism wherein the final predicted target span is randomly chosen from all predictions. As shown in Tab. 7, with our voting strategy to determine the best predicted target span, the performance of DiffusionVG gains a satisfactory improvement of 2.18% in R1@0.7. Even though all queries are targeted at recovering the same target span, it is important to consider that each prediction may exhibit a certain level of deviation. Our voting strategy aims to identify the common area among all predictions, while simultaneously mitigating their imprecise boundaries, thus results in the optimal localization of the target span.

Voting	R1@0.3	R1@0.5	R1@0.7
w/o	75.39	59.71	36.24
with	76.55	61.96	38.42

Table 7: **Voting strategy.** Impact of the post voting process on DiffusionVG.

C. Transformer Parameters

We exhibit the parameters in our Transformer model (video-centered encoder, span refining decoder and the DETR-like baselines of our implementation) in Tab. 8.

Parameter	Value
Encoder layers	4
Decoder layers	2
Attention heads	8
Dropout	0.1
Hidden dimension	256
FFN dimension	1024
Activation	ReLU

Table 8: Transformer parameters.

D. More Visualizations

We present more qualitative results on the test set of Charades-STA in Fig 8 to further analyze the specific mechanisms in our proposed DiffusionVG. Additionally, we visualize the sentence-to-video attention map from the last cross-attention layer of our video-centered multi-modal encoder. Based on these qualitative results, we summarized several noteworthy observations:

- (1) Our video-centered multi-modal encoder can precisely capture the intricate correlations between the sentence query and video representations, with the highest attention predominantly focused on the corresponding target moment within the video in most cases (1, 2, 3, 4).
- (2) The encoded multi-modal information is of vital importance since it provides indispensable guidance and serves as conditions for generating the target span through the denoising diffusion process. As shown in our failure case (6), the

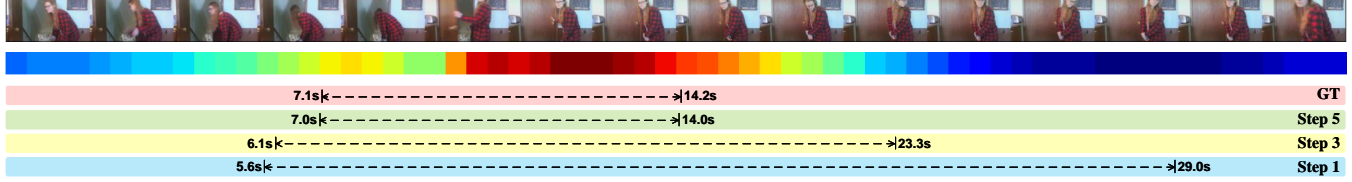
inaccurate attentions of the sentence query may result in deviations during the generation of the target span.

(3) Despite the significance of the accurate sentence-to-video attention, in cases where the error in the sentence-to-video attention remains within an acceptable range of deviation from the target moment, our DiffusionVG can effectively rectify the errors in attention within the denoising diffusion process, ultimately enabling precise span localization. As illustrate in case 5, the sentence-to-query attention from our video-centered encoder emphasizes on the middle part of the video, whereas the target moment is actually situated in the end of the video. However, by leveraging the inherent iterative refinement mechanisms of diffusion models, our DiffusionVG successfully generates the precise target moment. This observation further demonstrates the effectiveness of the iterative refining process in our DiffusionVG.

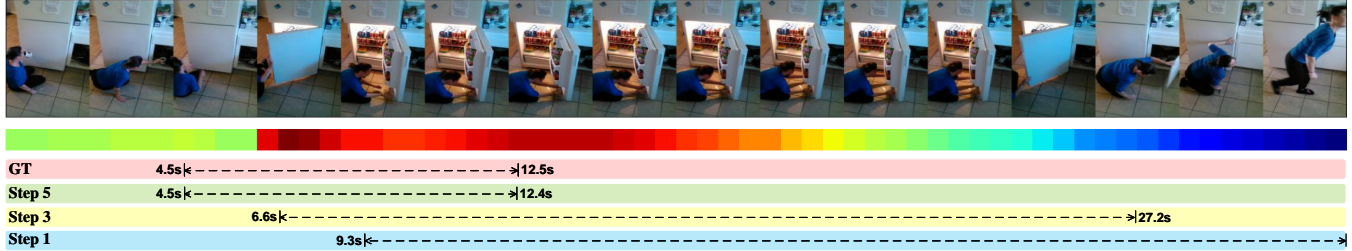
Query: A person begins tidying the table.



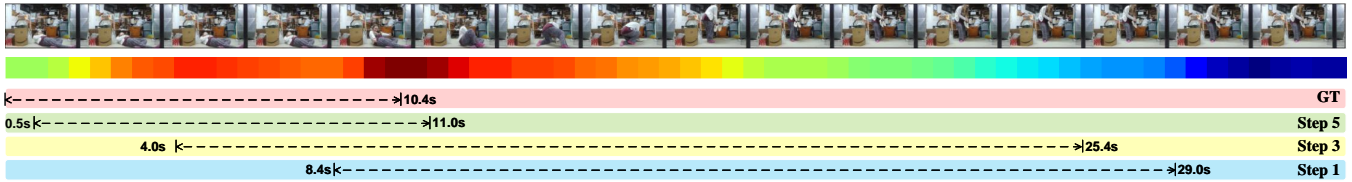
Query: A person is closing the door.



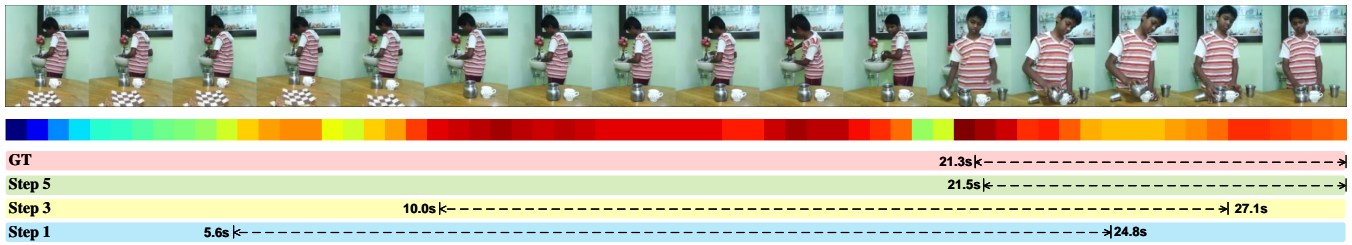
Query: The person is opening up a refrigerator.



Query: The person lays on the floor the gets up



Query: Person is pouring coffee into a cup in the dining room.



(Failure Case) Query: A person takes a book out from the entertainment center.

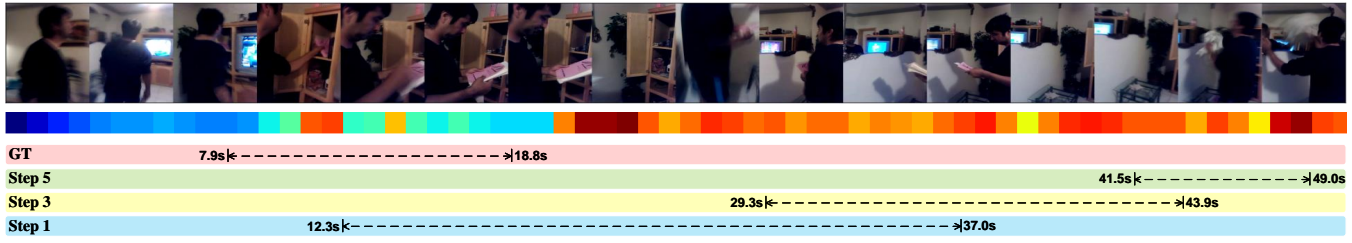


Figure 8: More visualized examples of our proposed DiffusionVG on Charades-STA test set. Additionally, we visualize the sentence-to-video attention map in each sample, where the average attention values for all words in a sentence are computed to yield the sentence-video level attentions.